IEEE Access
Multidisciplinary | Rapid Review | Open Access Journal

Received March 17, 2019, accepted April 12, 2019, date of publication April 16, 2019, date of current version April 29, 2019.

Digital Object Identifier 10.1109/ACCESS.2019.2911587

Multi-Timescale Active and Reactive Power-Coordinated Control of Large-Scale Wind Integrated Power System for Severe Wind Speed Fluctuation

JINXIN OUYANG, (Member, IEEE), MENGYANG LI, ZHEN ZHANG, AND TING TANG
State Key Laboratory of Power Transmission Equipment and System Security and New Technology, School of Electrical Engineering, Chongqing University, Chongqing 400044, China

Corresponding author: Jinxin Ouyang (sjinxinoy@163.com)

This work was supported in part by the National Natural Science Foundation of China under Grant 51877018, in part by the National Key Research and Development Plan under Grant 2017YFB0902005, and in part by the Science and Technology Project of State Grid under Grant SGXJ0000KXJS1700841.

ABSTRACT Wind speed fluctuations are extremely easy to cause the voltage change frequently. The existing voltage control methods are lacking in adjustment range and response speed. When wind speed fluctuates substantially or rapidly, voltage exceeding limit and the resulting grid safety problems cannot be avoided. Therefore, reasonably distributing and utilizing the reactive power of variable speed wind turbines in the whole network are an inevitable choice. However, the controllable reactive capacity of wind turbines is limited by converter capacity and active power, and thus, the grid demand may not be met. A new idea of active and reactive power-coordinated control for preventing voltage exceeding limit due to wind speed fluctuations was proposed. The effects of wind speed fluctuations on voltage were analyzed, and the controllable reactive capacity of variable speed wind turbines under wind speed fluctuations was studied. The relationship between voltage and the active and reactive power of wind farms was deduced. The theory and method of active and reactive power coordinated control before wind speed fluctuations were proposed based on the model predictive control theory. The control model based on multi-timescale was established. Finally, it was verified that the method can solve the voltage problems and maximize the system economy.

INDEX TERMS Wind power, wind speed fluctuation, voltage problem, active power control, reactive compensation.

I. INTRODUCTION

Wind power has been increasingly developed throughout the world for the past few years [1]. The active power output by wind turbine fluctuates with the wind speed fluctuations, therefore, the intrinsic randomness of wind energy will threaten the power balance of the power grid [2]. With the growing demand for renewable energy generation, wind power is developing to large-scale centralized construction. A regional power grid containing high-proportion wind power is generally connected to a load center through long-distance transmission lines, causing the support on the point of common connection (PCC) voltage is insufficient [3]. This problem will become more serious because of the rapid and random wind speed fluctuations [4].

The wind farm grid connection standard generally requires that wind farms must ensure the PCC voltage within an allowable range. Nowadays, a common measure for realizing this requirement is installing capacitors or reactors in the wind farms or integration substations, or regulating transformer tap [5], [6]. However, the change rate of voltage during wind speed fluctuations may be quite rapid, even more than 6kV within 10s in some wind farms [7]. Therefore, it may be difficult to control the PCC voltage within an allowable range by capacitors, reactors or transformer tap in the case of rapid wind speed fluctuations. Static var compensator (SVC), which can realize smooth and rapid reactive power adjustment, is more applicable [8]. However, it has been

The associate editor coordinating the review of this manuscript and approving it for publication was Enamul Haque.

investigated that the configured capacity of SVC is insufficient at present because of the expensive costs [9]. Historical data shows that the range of voltage fluctuation caused by wind fluctuation was more than 10% per day [7]. Therefore, it may be difficult to control the PCC voltage within an allowable range by SVC in the case of great wind speed fluctuations [10]. Moreover, SVC may cause voltage overshoot due to the hysteresis response, even leading to the cascading trip-off of the wind turbines [3], [11]. It further limits the application of SVC even without considering the costs.

For the wind farm owners, voltage exceeding limit influences wind turbines generate electricity normally and hinders wind turbines grid-connected operation, causing great economic losses. For power system operators, voltage exceeding limit caused by wind power may result in protection maloperation, equipment damage or even grid stability problems, bringing great security risks. As the installed capacity of wind power keeps increasing, the limitations of voltage control methods for wind power grid-connected power system are becoming increasingly serious.

Variable speed wind turbines (VSWTs) represented by permanent magnet synchronous generator (PMSG) and doubly fed induction generator (DFIG) have become the main equipment for wind power [3]. VSWTs can realize the decoupling control of active and reactive power by converter control. Therefore, the flexible and fast controllable reactive capability of VSWTs have become a reliable choice for solving the voltage problem of a grid-connected wind farms [12].

In recent years, the reactive power control of wind power system have received a lot of attentions, however, these researches mainly focused on the transient support of VSWTs for the voltage under grid fault [13]–[16]. However, the reactive control of wind turbines is not only employed for grid fault cases, but also for wind speed fluctuations. At present, there have been some studies on reactive control of variable speed wind turbines under normal operating conditions, and the voltage fluctuations have been proven greatly mitigated [7], [9], [17], [18]. Above methods for voltage control are realized by the reactive capacity of wind turbines, the reactive capacity is regarded as a fixed value determined by the converter capacity [19].

However, the reactive capacity of VSWT is influenced by its real-time active power. When the wind speed increases, the active power of VSWT increases while the reactive capacity decreases. Meanwhile, the reactive demand will increase as the voltage at the point of common connection (PCC) decreases. The reactive capacity could be unable to ensure the voltage within an accepted range if the wind speed fluctuates seriously. Therefore, when the voltage exceeding limit caused by wind speed fluctuations is unavoidable, it is an efficient method to beforehand adjust the active power of wind farms according to wind speed prediction, and reasonably distribute the active and reactive power of wind farms. Compared with the problems caused by over-limit voltage such as losing the grid-connected capability and decreasing the system security, the proposed method can perform better both in terms of economic and security. It should be noted that the control method proposed in this paper is only used for the cases that existing reactive capacities and control methods cannot ensure the PCC voltage within an allowable range.

To solve the voltage problems caused by wind speed fluctuations, a new control idea by coordinating active and reactive power was proposed. The effects of the active power of VSWTs on controllable reactive capacity and voltage were included. The active and reactive powers of VSWTs were optimized to prevent voltage exceeding the accepted range according to the wind speed prediction. This paper is reorganized as follows: Firstly, the effects of wind speed fluctuations on the grid voltage were analyzed; Secondly, the controllable reactive capacity of a VSWT under wind speed fluctuations was deduced; Subsequently, the relationship between voltage and active and reactive powers of VSWTs was deduced; Then, the idea and method for voltage control by coordinating the active and reactive power was proposed, and the multi time-scale control model based on model predictive control theory (MPC) was established; Finally, the effectiveness of this method was demonstrated by using examples.

II. POWER-VOLTAGE CHARACTERISTICS OF WIND POWER SYSTEM

A. INFLUENCES OF WIND SPEED FLUCTUATIONS

As the wind speed fluctuates, the active power of wind machine will fluctuate as well. The active power output by DFIG is approximately equal to the mechanical power because the converter and internal losses are small enough to be neglected [20], which can be written as [21]

$$P_D = 0.5\rho\pi R^2 v_{\mathrm{w}}^2 C_{\mathrm{pmax}}(1+s) \tag{1}$$

where ρ is air density, R is blade radius of wind machine, v_w is wind speed, s is slip ratio, and C_{pmax} is the maximum rotor power coefficient.

The converter and internal losses of PMSG are small enough to be neglected as similar with DFIG. The maximum active power output by PMSG at one wind speed is equal to the mechanical power because the wind machine is directly connected to the drive shaft. Therefore, the active power of PMSG is written as

$$P_P = 0.5\rho\pi R^2 v_{\mathrm{w}}^3 C_{\mathrm{pmax}} \tag{2}$$

A power system contained with m wind farms is shown in Figure 1, where $B2$ is the PCC, $T1$ is the booster station, and the line from $B2$ to $B3$ is the AC transmission lines. Moreover, the reactive power compensators are installed at $B1$. The active and reactive powers from VSWTs flow past $B1$, and converge together with the reactive power of compensators. Then, the powers from $B1$ flow past $T1$ and transmit to the grid.

The relationship between the voltage at PCC and $B1$ and the active and reactive power of the power system in Figure 1

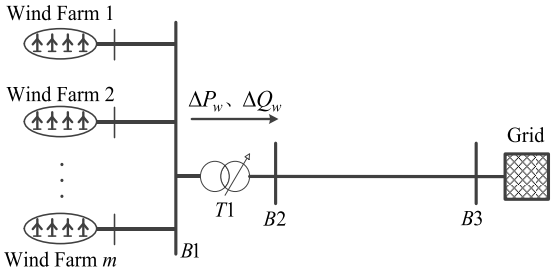

FIGURE 1. A power system with m wind farms.

can be expressed as [22]

$$\begin{bmatrix} \Delta U_{\mathrm{pcc}} \\ \Delta U_{\mathrm{B1}} \end{bmatrix} = \mathbf{\Gamma_{us}} \begin{bmatrix} \Delta P_{\mathrm{w}} \\ \Delta Q_{\mathrm{w}} \end{bmatrix} \tag{3}$$

where ΔU_{pcc} is the PCC voltage variation, ΔU_{B1} is the voltage variation at $B1$, ΔP_w and ΔQ_w are the active and reactive power variations passing through $T1$ respectively, and $\mathbf{\Gamma_{us}}$ is the sensitivity matrix of voltage-power, which is

$$\mathbf{\Gamma_{us}} = \begin{bmatrix} a_{11} & a_{12} \\ a_{21} & a_{22} \end{bmatrix} \tag{4}$$

where a_{11} and a_{12} are the sensitivities of PCC voltage to active and reactive power passing through the booster station respectively, a_{21} and a_{22} are the sensitivities of $B1$ voltage to active and reactive power passing through the booster station respectively.

Therefore, the active power of VSWT varies with the wind speed fluctuations, resulting in the PCC voltage fluctuations. The reactive compensation devices and wind turbines respond, causing reactive power flow changes and further affecting the grid voltage. Voltage variations under wind speed fluctuations are depended on the reactive power of the reactive compensation devices and the active and reactive power of wind turbines.

B. CONTROLLABLE REACTIVE CAPACITY OF VSWT

The reactive power of DFIG is the sum of stator and grid-side converter reactive power. Considering the limit of grid-side converter capacity and rotor current, the controllable reactive capacity of DFIG is [23]

$$Q_{D.\max} = \sqrt{R_{\mathrm{sc}}^2 - (P_{\mathrm{Ds}} - P_{\mathrm{sc}})^2} - Q_{\mathrm{sc}} + \sqrt{S_{\mathrm{Dc}}^2 - (sP_{\mathrm{Ds}})^2} \tag{5}$$

In Equation (5),

$$P_{\mathrm{sc}} = \frac{3U_{\mathrm{sm}}^2 R_{\mathrm{s}}}{2\left(R_{\mathrm{s}}^2 + X_{\mathrm{s}}^2\right)} \tag{6}$$

$$Q_{\mathrm{sc}} = \frac{3U_{\mathrm{sm}}^2 X_{\mathrm{m}}}{2\left(R_{\mathrm{s}}^2 + X_{\mathrm{s}}^2\right)} \tag{7}$$

$$R_{\mathrm{sc}}^2 = \frac{9U_{\mathrm{sm}}^2 X_{\mathrm{m}}^2}{4\left(R_{\mathrm{s}}^2 + X_{\mathrm{s}}^2\right)} I_{\mathrm{rmax}}^2 \tag{8}$$

where I_{rmax} is the maximum current of rotor, U_{sm} is the amplitude of stator voltage, P_{Ds} is the active power of DFIG stator, R_s and X_s are the stator resistance and reactance respectively, X_{m} is the magnetizing reactance, S_{Dc} is the grid-side converter capacity. The power controllable range on stator side is a circle with the center of (P_{sc}, Q_{sc}) and the radius R_{sc}.

The controllable reactive power of PMSG is influenced by its converter capacity. Therefore, the reactive power capacity of PMSG can be written as

$$Q_{\mathrm{P.max}} = \sqrt{S_{\mathrm{Pc}}^2 - P_{\mathrm{P}}^2} \tag{9}$$

where S_{Pc} is the capacity of grid-side converter of PMSG, and P_{P} is the active power.

Under wind speed fluctuations, PCC voltage variation should be limited into an accepted range. According to Equation (3), the reactive demand of ensuring the PCC voltage within an acceptable range can be written as

$$\Delta Q_{\mathrm{w,de}} = \frac{\Delta U_{\mathrm{pcc,al}} - a_{11}\left(N_{\mathrm{D}}\Delta P_{\mathrm{D}} + N_{\mathrm{P}}\Delta P_{\mathrm{p}}\right)}{a_{12}} \tag{10}$$

where $\Delta U_{\mathrm{Pcc,al}}$ is the maximum allowable variation on PCC, N_{D} and N_{P} are the number of DFIG and PMSG respectively, ΔP_{D} and ΔP_{P} are the active power variation of DFIG and PMSG respectively.

The reactive control of DFIG and PMSG can quickly respond to voltage variation and make up for voltage variation due to wind speed fluctuation [24], [25]. However, the controllable reactive power of a wind farm is the sum of the reactive capacity of all VSWTs. The reactive capacities of VSWTs depend on their active power, which may be unable to limit the PCC voltage into an accepted range.

III. CONTROL IDEA OF COORDINATING ACTIVE AND REACTIVE POWER

Wind speed fluctuations affect grid voltage through active power directly and through the reactive power indirectly. The reactive control of VSWTs is an effective measure to make up for voltage variations. Moreover, the controllable reactive capacity of wind farms can be improved and the voltage can be limited into an acceptable range by adjusting the active power of VSWTs proactively [26]. Therefore, the effects of active and reactive power should be considered for controlling the grid voltage under the wind speed fluctuations.

Equation (11) can judge whether the reactive demand of limiting the PCC voltage into an acceptable rang can be met.

$$\Delta Q_{\mathrm{w,de}} - \Delta Q_{\mathrm{c,max}} \le N_{\mathrm{D}} Q_{\mathrm{D.\,max}} + N_{\mathrm{p}} Q_{\mathrm{p.\,max}} \tag{11}$$

where $\Delta Q_{\mathrm{c,max}}$ is the maximum adjustment range of reactive power compensation devices.

When the controllable reactive power of grid cannot meet the system demand, the active power of VSWTs is adjusted before the wind speed fluctuations to improve the reactive power capacity. The active power of grid is usually ample; thus, the reduced active power of wind farms can be compensated through the coordination of power grid. Therefore, the controllable reactive capacity of VSWTs can be improved

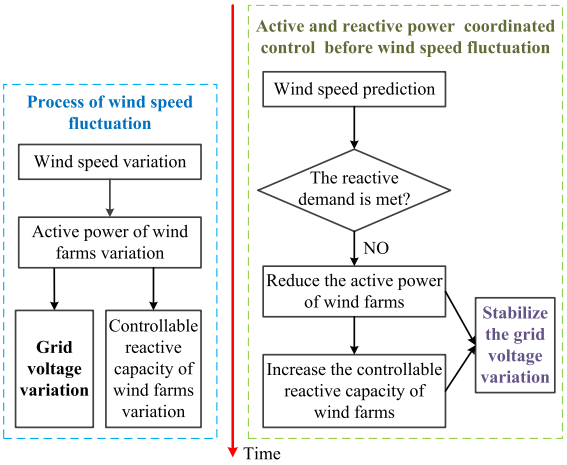

FIGURE 2. Active and reactive power-coordinated control.

by reducing the active power. When the wind speed fluctuates seriously, the measure can be used for the rapid voltage control. The control theory of coordinating active and reactive power is shown in Figure 2.

If Equation (11) is not satisfied, the controllable reactive capacity of the wind power system is insufficient. Thus, VSWTs should be controlled at the reactive power limit. The PCC voltage can be expressed as

$$U_{\mathrm{pcc}} = a_{12}N_{\mathrm{D}}\left[\sqrt{R_{\mathrm{sc}}^2-\left(\frac{P_{\mathrm{D}}}{s+1}-P_{\mathrm{sc}}\right)^2}-Q_{\mathrm{sc}}+\sqrt{S_{\mathrm{Dc}}^2-\left(\frac{sP_{\mathrm{D}}}{s+1}\right)^2}\right]+a_{12}N_{\mathrm{P}}\left(\sqrt{S_{\mathrm{Pc}}^2-P_{\mathrm{P}}^2}\right)+a_{11}\left(N_{\mathrm{D}}P_{\mathrm{D}}+N_{\mathrm{P}}P_{\mathrm{P}}\right)+M_2 \tag{12}$$

In Equation (12),

$$M_2 = U'_{\mathrm{pcc}} - a_{11}\left(N_{\mathrm{D}}P'_{\mathrm{D}}+N_{\mathrm{P}}P'_{\mathrm{P}}\right)+a_{12}Q_{c,\max} - a_{12}\left(Q'_{\mathrm{c}}+N_{\mathrm{D}}Q'_{\mathrm{D}}+N_{\mathrm{P}}Q'_{\mathrm{P}}\right) \tag{13}$$

where U'_{pcc} is the PCC voltage before power variation, Q'_{D} and P'_{D} are the reactive and active power of DFIG before power variation, P'_{P} and Q'_{P} are the active and reactive power of PMSG before power variation respectively.

Figure 3 shows the relationship between PCC voltage and active power of VSWTs. PCC voltage is a non-monotonic function of the active power of DFIG and PMSG. According to Equation (12), U_{pcc} changes linearly with N_{D} or N_{P}, so the change rules of U_{pcc} under any N_{D} and N_{P} are same to the Figure 3. Therefore, whatever the value of N_{D} and N_{P} are, under the premise of satisfying the active power flow balance and voltage within allowable range, there is an optimum value which can maximize the active power of VSWTs.

Under the same load, the greater the active power of VSWTs is, the smaller the active power of thermal power units and the better the grid economy are. Therefore, the

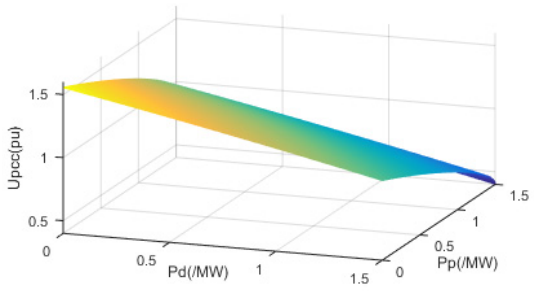

FIGURE 3. Relationship between PCC voltage and active power of VSWTs.

reduction in the active power of VSWTs should be minimized. The active power of VSWTs affects the grid voltage directly, although it affects grid voltage indirectly through the controllable reactive capacity of wind farms. Therefore, the active and reactive power of VSWTs must be coordinated to limit the grid voltage into an allowable range while maximizing the power system economy.

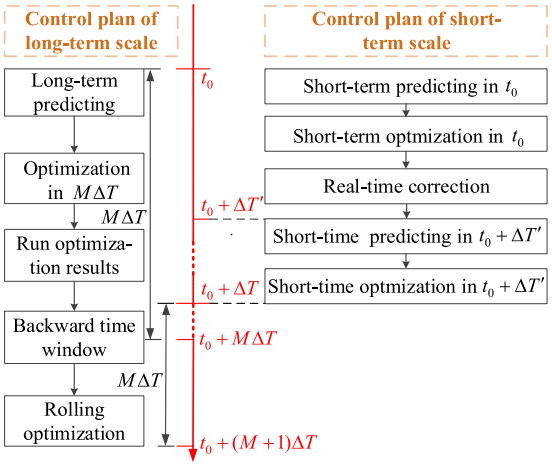

FIGURE 4. Multi time-scale control based on MPC.

The uptime and off-time of thermal power units are limited, and switching capacitors is difficult to meet the response speed requirements under rapid wind speed fluctuation. Therefore, thermal power units and capacitors can hardly realize short-term or real-time control. However, the prediction error of wind speed is large under long-term scale, resulting in large control errors. Therefore, a multi-timescale active and reactive power-coordinated control strategy before wind speed fluctuation based on MPC is proposed. Figure 4 shows the multi-timescale control theory based on MPC. The relationship between long-term optimization control and short-term control is:

1) Long-term optimization control is mainly used to determine the switching states of capacitors and the combination of thermal power units in grid, which will not change in the short-term scale. The long-term control objective is to minimize the generating costs of thermal power units, which includes operating and start-up costs. Long-term control starts at every ΔT time interval and predicts wind power and

load in future $M\Delta T$ periods. However, each power supply only executes the power plan at the first moment. At the next moment $t_0+\Delta T$, the time window moves backward by a time interval, and the above process is repeated.

2) Short-term optimization control is mainly used to determine the actual power of each power supply. The short-term control objective is to minimize the operating cost of thermal power units. The sampling step-size of short-term control is $\Delta T'$ ($\Delta T' < \Delta T$), the actual power of each power supply will be corrected in real time. Then repeat the process of short-term control until at the next sampling moment of long-term control.

The MPC technology can obtain an optimized control sequence through considering comprehensively the predicted data and the current operating status of the power grid. According to the wind speed prediction, the active and reactive power of VSWTs and thermal power units are optimized online based on MPC. Therefore, the grid voltage can be limited into an allowable range and the operating costs of the power system is lowest.

IV. CONTROL MODEL BASED ON COORDINATING ACTIVE AND REACTIVE POWER

A. LONG-TERM CONTROL MODEL

The control variables of long-term scale include active and reactive power of each thermal power unit and each wind farm, reactive compensation of capacitors, and reactive power of SVCs. The control model optimizes the above control variables according to the long-term wind speed prediction. The system economy can be expressed by the generating costs $f_1$of all thermal power units, which include operating and start-up costs. Wind power consumption is maximized by adding a penalty termf_2 of abandoning wind to the objective function, which has the following expression:

$$F_1 = \min\left(f_1 + f_2\right) \tag{14}$$

$$f_1 = \sum_{\mathrm{t}=1}^{N_\mathrm{t}} \sum_{\mathrm{i}=1}^{N_\mathrm{G}} \left[U_{\mathrm{i.t}} \left(a_\mathrm{i} P_{\mathrm{G.i.t}}^2 + b_\mathrm{i} P_{\mathrm{G.i.t}} + c_\mathrm{i} \right) + B_{\mathrm{i.t}} S_\mathrm{i} \right] \tag{15}$$

$$f_2 = \sum_{\mathrm{t}=1}^{N_\mathrm{t}} \sum_{\mathrm{i}=1}^{N_\mathrm{w}} C_\mathrm{w} \left(\tilde{P}_{\mathrm{w.k.t}} - P_{\mathrm{w.k.t}} \right) \tag{16}$$

where $t = 1, 2, \ldots, N_\mathrm{t}$, N_t is the number of time interval under long-term scale, $i = 1, 2, \ldots, N_\mathrm{G}$, N_G is the number of thermal power units, $B_{\mathrm{i.t}} = \max\left(U_{\mathrm{i.t}} - U_{\mathrm{i.t\text{-}1}}, 0\right)$, $U_{\mathrm{i.t}}$ is the 1-0 variable indicating the i-th thermal power unit operating or not at time t, $B_{\mathrm{i.t}}$ is the 1-0 variable indicating the i-th thermal power unit switching on or not, $P_{\mathrm{G.i.t}}$ is the active power of the i-th thermal power unit at time t, is the start-up cost of the i-th thermal power unit, C_w is the cost coefficient of abandoning wind, a_i, b_i and c_i are characteristic parameters of energy dissipation, $\tilde{P}_{\mathrm{w.k.t}}$ and $P_{\mathrm{w.k.t}}$ are the predicted and actual active power of the k-th wind farm respectively.

The long-term control model has the following constraints:

1) Constraint of system power balance

$$\begin{cases} P_{\mathrm{L.t}} = \sum_{\mathrm{i}=1}^{N_\mathrm{G}} U_{\mathrm{i.t}} P_{\mathrm{G.i.t}} + \sum_{\mathrm{k}=1}^{N_\mathrm{w}} P_{\mathrm{w.k.t}} \\ Q_{\mathrm{L.t}} = \sum_{\mathrm{i}=1}^{N_\mathrm{G}} U_{\mathrm{i.t}} Q_{\mathrm{G.i.t}} + \sum_{\mathrm{k}=1}^{N_\mathrm{w}} Q_{\mathrm{w.k.t}} + Q_{\mathrm{c.t}} + Q_{\mathrm{svc.t}} \end{cases} \tag{17}$$

where $P_{L.t}$ and $Q_{L.t}$ is the active and reactive load of grid under long-term scale respectively, $Q_{G.i.t}$ is the reactive power of the i-th thermal power unit at time t under long-term scale, $P_{w.k.t}$ and $Q_{w.k.t}$ are the active and reactive power of the k-th wind farm at time $t$under long-term scale respectively, $Q_{c.t}$ and $Q_{svc.t}$ are the reactive power of capacitors and SVCs at time $t$under long-term scale respectively.

2) Power constraint of wind farm

$$\begin{cases} 0 \le P_{\mathrm{w.k.t}} \le \tilde{P}_{\mathrm{w.k.t}} \\ Q_{\mathrm{w.k.t}} \le Q_{\mathrm{w.k}}^{\max} \end{cases} \tag{18}$$

where $Q_{\mathrm{w.k}}^{\max}$ is the controllable reactive capacity of the k-th wind farm under the predicted active power.

3) Power constraint of thermal power unit

$$\begin{cases} P_{\mathrm{G.i.t}}^{\min} \le P_{\mathrm{G.i.t}} \le P_{\mathrm{G.i.t}}^{\max} \\ |Q_{\mathrm{G.i.t}}| \le \sqrt{\left(S_{\mathrm{G.i}}^N\right)^2 - \left(P_{\mathrm{G.i.t}}\right)^2} \end{cases} \tag{19}$$

where $P_{\mathrm{G.i.t}}^{\max}$ and $P_{\mathrm{G.i.t}}^{\min}$ are the allowable maximum and minimum active power of the i-th thermal power unit respectively, $S_{\mathrm{G.i}}^N$ is the rated apparent power of the i-th thermal power unit.

4) Climbing ability constraint of thermal power unit

$$\begin{cases} P_{\mathrm{G.i.t}} - P_{\mathrm{G.i.t\text{-}1}} \le U_{\mathrm{i.t\text{-}1}} R_{\mathrm{u.t}} + (1 - U_{\mathrm{i.t\text{-}1}}) P_{\mathrm{G.i}}^{\max} \\ P_{\mathrm{G.i.t}} - P_{\mathrm{G.i.t}} \le U_{\mathrm{i.t}} R_{\mathrm{d.i}} + (1 - U_{\mathrm{i.t}}) P_{\mathrm{G.i}}^{\max} \end{cases} \tag{20}$$

where $R_{u.i}$ and $R_{d.i}$ are the climbing speed and landslide speed of the i-th thermal power unit respectively.

5) Minimum starting-up and shutdown time constraint of thermal power unit

$$\begin{cases} (T_{i.t-1}^{on} - T_{i.\min}^{on})(U_{i.t-1} - U_{i.t}) \ge 0 \\ (T_{i.t-1}^{off} - T_{i.\min}^{off})(U_{i.t-1} - U_{i.t}) \ge 0 \end{cases} \tag{21}$$

where $T_{i.t-1}^{on}$ and $T_{i.t-1}^{off}$ are the durations of on/off state of the i-th thermal power unit respectively at time t-1, $T_{i.\min}^{on}$ and $T_{i.\min}^{off}$ are the minimum durations of on/off state of the i-th thermal power unit respectively.

6) Reactive power constraint of capacitor and SVC

$$0 \le Q_{\mathrm{c.t}} \le Q_{\mathrm{c.max}} \tag{22}$$

$$0 \le Q_{\mathrm{svc.t}} \le Q_{\mathrm{svc.max}} \tag{23}$$

where $Q_{\mathrm{c.max}}$ and $Q_{\mathrm{svc.max}}$ are the maximum reactive power of capacitors and SVCs respectively.

7) Voltage constraint at PCC

$$U_{\mathrm{pcc.min}} \le U_{\mathrm{pcc.t}} \le U_{\mathrm{pcc.max}} \tag{24}$$

where $U_{\mathrm{pcc.t}}$ calculated by Equation (3) is the PCC voltage at time t under long-term scale, $U_{\mathrm{pcc.max}}$ and $U_{\mathrm{pcc.min}}$ are the upper and lower limit of PCC voltage respectively.

B. SHORT-TERM CONTROL MODEL

The on/off state of thermal power units and capacitors are determined under long-term optimization control. The control variables of short-term scale include: active and reactive power of each thermal power unit, active and reactive power of each wind farm, and reactive power of SVCs. The above control variables are optimized on the basis on short-term wind speed prediction. The short-term control objective is minimizing the operating cost of thermal power units. Under the short-time scale, wind farms can increase the wind power consumption capacity by abandoning wind [27], so there is no penalty term in this objective function. The expression of F_2 is:

$$F_2 = \min \sum_{\mathrm{i}=1}^{N_\mathrm{G}} \left[U_{\mathrm{i.t}} \left(a_\mathrm{i} {P'_{\mathrm{G.i.t}}}^2 + b_\mathrm{i} P'_{\mathrm{G.i.t}} + c_\mathrm{i} \right) \right] \tag{25}$$

where $P'_{\mathrm{G.i.t}}$ is the active power of the i-th thermal power unit under short-term scale.

The short-term control model has the following constraints:

1) Constraint of system power balance

$$\begin{cases} P'_{\mathrm{L.t}} = \sum_{\mathrm{i}=1}^{N_\mathrm{G}} U_{\mathrm{i.t}} P'_{\mathrm{G.i.t}} + \sum_{\mathrm{k}=1}^{N_\mathrm{w}} P'_{\mathrm{w.k.t}} \\ Q'_{\mathrm{L.t}} = \sum_{\mathrm{i}=1}^{N_\mathrm{G}} U_{\mathrm{i.t}} Q'_{\mathrm{G.i.t}} + \sum_{\mathrm{k}=1}^{N_\mathrm{w}} Q'_{\mathrm{w.k.t}} + Q_{\mathrm{c.t}} + Q'_{\mathrm{svc.t}} \end{cases} \tag{26}$$

where $P'_{\mathrm{L.t}}$ and $Q'_{\mathrm{L.t}}$ is the active and reactive load of grid under short-term scale respectively, $Q'_{\mathrm{G.i.t}}$is the reactive power of the i-th thermal power unit at time $t$under short-term scale, $P'_{\mathrm{w.k.t}}$ and $Q'_{\mathrm{w.k.t}}$ are the active and reactive power of the k-th wind farm at time $t$under short-term scale respectively, $Q'_{\mathrm{svc.t}}$ are the reactive power of capacitors and SVCs at time t.

2) Power constraint of wind farm

$$\begin{cases} 0 \le P'_{\mathrm{w.k.t}} \le \tilde{P}'_{\mathrm{w.k.t}} \\ Q'_{\mathrm{w.k.t}} \le Q^{\max}_{\mathrm{w.k}} \end{cases} \tag{27}$$

where $\tilde{P}'_{\mathrm{w.k.t}}$ is the predicted active power of the k-th wind farm at time t under short-term scale.

3) Power constraint of thermal power unit

$$\begin{cases} P^{\min}_{\mathrm{G.i.t}} \le P'_{\mathrm{G.i.t}} \le P^{\max}_{\mathrm{G.i.t}} \\ |Q'_{\mathrm{G.i.t}}| \le \sqrt{\left(S^N_{\mathrm{G.i}}\right)^2 - \left(P'_{\mathrm{G.i.t}}\right)^2} \end{cases} \tag{28}$$

4) Reactive power constraint of SVC

$$0 \le Q'_{\mathrm{svc.t}} \le Q_{\mathrm{svc.max}} \tag{29}$$

5) Voltage constraint at PCC

$$U_{\mathrm{pcc.min}} \le U'_{\mathrm{pcc.t}} \le U_{\mathrm{pcc.max}} \tag{30}$$

where $U'_{\mathrm{pcc.t}}$ calculated by Equation (3) is the PCC voltage at time t under short-term scale.

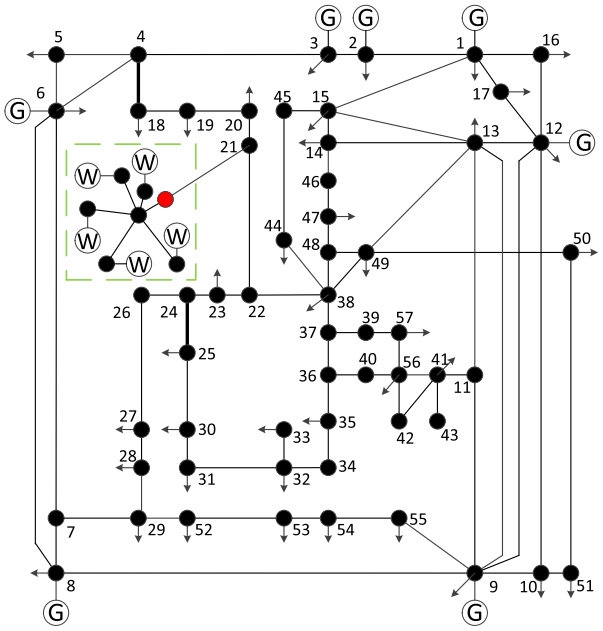

FIGURE 5. The system diagram of examples.

V. EXAMPLES

For verifying the validity of active and reactive power-coordinated control method, an example of 5 wind farms integrated into a standard IEEE57 system is built. Figure 5 shows the system diagram, where the red node represents the point of common connection. The total installed capacity of all VSWTs is 225 MW, and the length of the AC transmission line between PCC to the IEEE57 system is 40 km. The capacitor capacity of hosting wind farms is 35Mvar, and the SVC capacity is 250Mvar. The five wind farms consist of 80 DFIG and 70 PMSG. The capacity of a VSWT is 1.5 MW, and the rated wind speed is 15 m/s.

There are 7 thermal power units in the IEEE57 system. Table 1 lists the active power limit and the cost coefficients of each unit, and number of each unit is the conjoint node ID. The No. 1 thermal power unit is a balancing unit.

TABLE 1. Unit parameters in IEEE57 node system.

Unit	Upper limit of active power(/MW)	Lower limit of active power(/MW)	a	b	c
1	578.55	300	75	200	0
2	100	40	350	175	0
3	140	50	1250	100	0
6	100	40	166	325	0
8	550	300	75	200	0
9	100	40	500	300	0
12	200	60	500	300	0

Under the wind speed fluctuations, the multi-time rolling optimization based on MPC is used, and the influences of three models are compared. The control step-sizes of long-term and short-scale are 15 and 5min, respectively. The particle swarm optimization is adopted in the three models, and the model is introduced as follows.

In the first model, abandoning wind is not considered in wind farms, that is, the active power of VSWTs is based on the real-time prediction. The optimization objective of the first model is minimizing the generating costs of thermal power units. In the second model, abandoning wind is considered, that is, the controllable reactive capacity of all VSWTs can be increased by decreasing active power according to the wind speed prediction. However, the influences of active power of VSWTs on PCC voltage are not considered. The optimization objective of the second model is minimizing the generating costs of thermal power units under ensuring the voltage within an allowable range. The third model is the active and reactive power-coordinated control strategy proposed in this paper. In the third model, wind farms are allowed abandoning wind, and the influences of active and reactive power on PCC voltage are considered. The optimization objective of the third model is minimizing the generating costs of thermal power units under ensuring the voltage within an allowable range. In all models, the reactive power compensation quantities of capacitors and SVCs are considered.

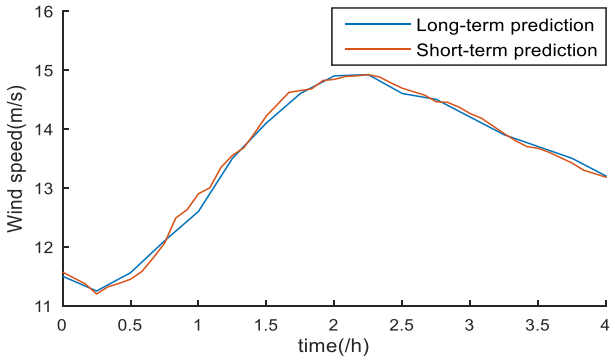

FIGURE 6. Wind speed variations under multi-timescale.

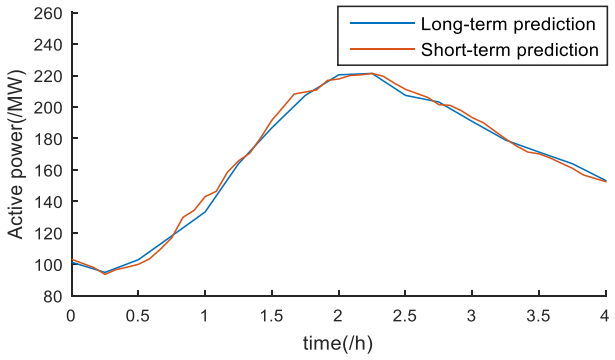

FIGURE 7. Active power predictions of wind farms under multi-timescale.

Figure 6 shows wind speed at different times under multi-timescale. Figure 7 shows the active power predictions of all VSWTs based on the above wind speed. Figure 8 shows the active load of grid within 4 h under multi-timescale. As shown in Figures 6 and 7, the active powers of VSWTs increase as the wind speed increases.

The amplitude of PCC voltage under the three model is shown in Figure 9. PCC voltage is able to maintain 1.0 pu when the reactive power demand of the power system is met.

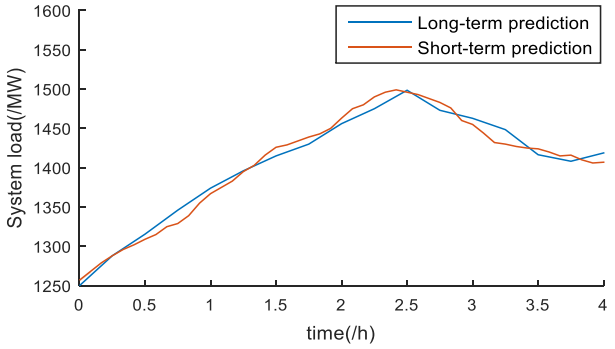

FIGURE 8. Active load predictions of the system under multi-timescale.

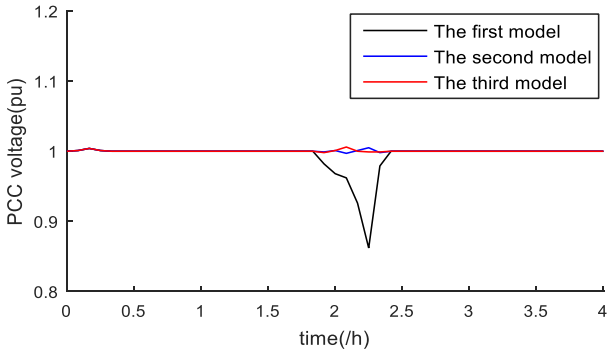

FIGURE 9. Amplitude of PCC voltage under the three models.

At 5–15 min, PCC voltage is slightly larger than 1.0 pu, because the reactive power of the capacitors determined under long-term scale, which cannot be changed under short-term scale, is larger than the reactive power demand under short-term scale. At 115–140 min, wind speed increases to nearly 15m/s, and the PCC voltage drops to approximately 0.862 pu under the first model. Therefore, wind speed fluctuation will damage the grid voltage if the voltage control methods are not taken. When the control method of the second and third models are considered, PCC voltage can be kept between 0.997 and 1.007 pu.

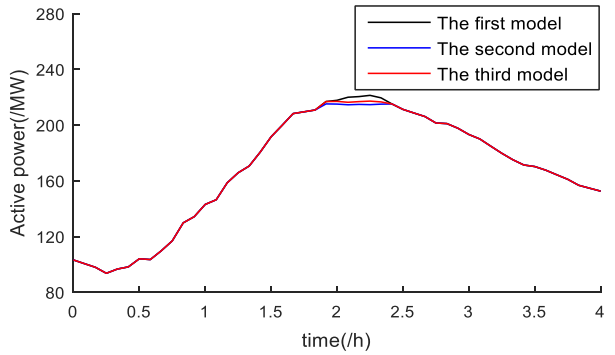

FIGURE 10. Active power of wind farms under three models.

Figures 10 and 11 are the active and reactive power of variable speed wind turbines respectively at different times under the three models. As shown in Figure 10, when taking the first model, the active power of variable speed wind turbines is equal to the active power prediction under short-term

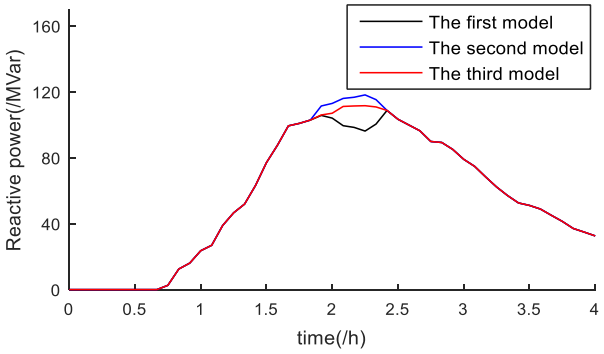

FIGURE 11. Reactive power of wind farms under three models.

scale, and the active power of the second model was the smallest. At 115–140 min, when taking the second and third models, variable speed wind turbines proactively reduce active power to increase the controllable reactive capacity. Hence, the active power of variable speed wind turbines is smaller than the first model. As shown in Figure 11, at 0–40 min, the reactive demand of PCC can be met by capacitors and SVCs, and thus variable speed wind turbines do not output reactive power. As the wind speed increases, capacitors and SVCs fail to meet reactive power demand, and variable speed wind turbines need to output reactive power to compensate for the reactive power deficits. At 115–140 min, when taking the first model, wind farms output reactive power depends on the controllable reactive capacity. When the second and third models are considered, the reactive power of the variable speed wind turbines increases and the second model has the largest reactive power. As shown in Figures 9 to 11, the second and third models improved the controllable reactive capacity of wind farms by reducing active power, providing sufficient reactive support for grid to meet the voltage demand. However, the influences for active power of wind farms on grid voltage are considered under the third model. This condition conforms to the actual state and improves the active power of wind farms.

Figure 12 compares the active power of thermal power units under the three models. As shown in Figure 12 (a), the active power of units #2, #3, #6, #9, and #12 under the three models are in agreement. The unit #3 is full load at all times, #6 and #9 always remain off, #12 always output power of 60 MW, and #2 changes from 100 MW to 0 MW at 3 h. Therefore, the differences in the active power of units under the three models are only in #1 and #8. Figure 12 (b) compares the active power of thermal power units #1 and #8 in the three models. At 115–140 min, the second and third models reduce the active power of VSWTs to limit PCC voltage into an allowable range. Hence, increasing the active power of thermal power units is necessary to compensate for the deficit of active power. Units #1 and #8 are adjusted for to maximize economy of the power system. Figure 12 indicates the active power of thermal power units in the second model is more than that of the third model. Therefore, the third model can limit the PCC voltage into allowable range through small economic losses.

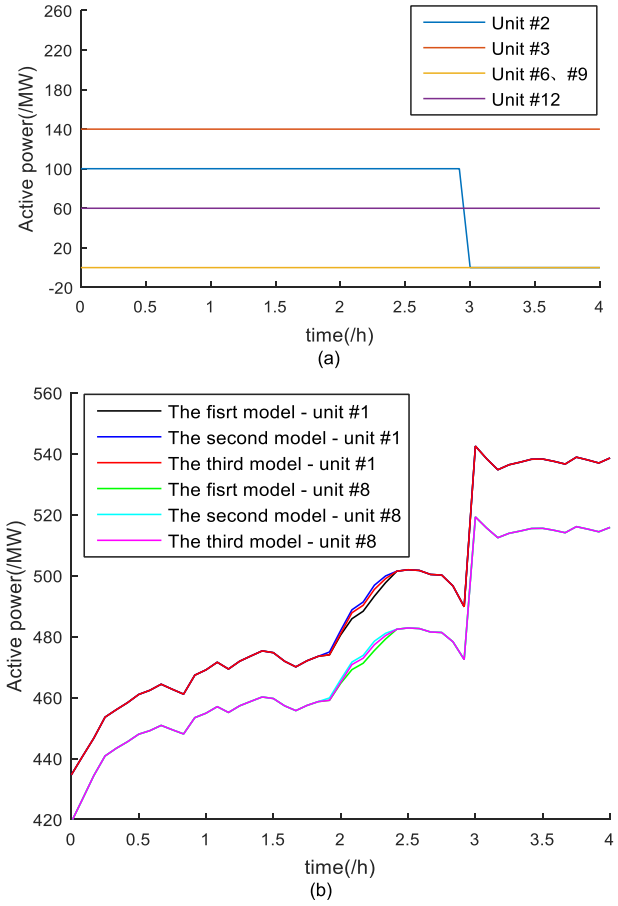

FIGURE 12. Active power of thermal power units under three models (a) units #2, #3, #6, #9 and #12 (b) units #1 and #8.

TABLE 2. Costs under three models.

Model	Abandon wind indicators		Costs
	Power (MW)	Ratio (%)	
The first model	0	0	12.2366
The second model	26.6292	2.02	12.2175
The third model	15.0652	1.14	12.1925

The abandoning wind indicators of VSWTs and the total costs of thermal power units under the three models are shown in Table 2. It can be seen from Table 2 that the abandoning wind ratio of the second model is higher than the third model. Furthermore, the generating costs of thermal power units under the first model is the highest, and the model proposed in this paper has the lowest power generation costs

VI. CONCLUSION

The reactive control of VSWT is an effective measure to make up for voltage variation under wind speed fluctuation. However, the controllable reactive capacity of wind farms, which depends on active power, may be unable to limit PCC voltage into allowable range. Furthermore, voltage can be influenced to an extent by changing active power. Therefore, the influence of active and reactive power of wind farms on grid voltage should be considered.

In this paper, the new idea of voltage control was proposed based on coordinating active and reactive power before the wind speed fluctuations. According to the wind speed prediction and the sensitivity matrix, the grid voltage was limited into an allowable range by adjusting the active power of VSWTs in advance and fully excavating the controllable reactive capability of VSWTs. The active and reactive power of VSWTs and the grid were optimized under the control objective of maximizing the power system economy and the constraints of voltage, power flow, power supply and so on. The method can effectively improve the contradiction between the influence of wind speed fluctuation on voltage and the limitation of controllable reactive power capacity of wind turbine through a small amount of wind abandonment. The examples in this paper have verified that the control method can quickly and effectively prevent the voltage problems and realize the safe and economical operation of the grid under the rapid and serious fluctuations of wind speed.

Compared with the method ignoring the influences of active power of VSWTs on PCC voltage, the control strategy proposed in this paper can limit the voltage into an allowable range by lesser economic loss of the wind power system. Coordinating the active and reactive power of wind farms and grid in advance is significant for the safe and stable operation of wind power system.

REFERENCES

[1] F. Bai *et al.*, "A measurement-based approach for power system instability early warning," *Protection Control Mod. Power Syst.*, vol. 1, no. 4, pp. 1–9, Jun. 2016.

[2] J. O. G. Tande, "Impact of wind turbines on voltage quality," in *Proc. 8th Int. Conf. Harmon. Qual. Power*, vol. 2, Oct. 1998, pp. 1158–1161.

[3] J. Ouyang, M. Li, Y. Diao, T. Tang, and Q. Xie, "Active control method of large-scale wind integrated power system with enhanced reactive power support for wind speed fluctuation," *IET Gener., Transmiss. Distrib.*, vol. 12, no. 21, pp. 5664–5671, Nov. 2018.

[4] Y. Zhang, T. Ye, Y. Xin, F. Han, and G. Fan, "Problems and measures of power grid accommodating large scale wind power," *Proc. CSEE*, vol. 30, no. 25, pp. 1–9, Sep. 2010.

[5] S. Saad and L. Zellouma, "Fuzzy logic controller for three-level shunt active filter compensating harmonics and reactive power," *Electr. Power Syst. Res.*, vol. 79, no. 10, pp. 1337–1341, Oct. 2009.

[6] H. Myneni, G. S. Kumar, and D. Sreenivasarao, "Dynamic dc voltage regulation of split-capacitor DSTATCOM for power quality improvement," *IET Gener., Transmiss. Distrib.*, vol. 11, no. 17, pp. 4373–4383, Nov. 2017.

[7] Q. Guo, H. Sun, B. Wang, B. Zhang, W. Wu, and L. Tang, "Hierarchical automatic voltage control for integration of large-scale wind power: Design and implementation," *Electr. Power Syst. Res.*, vol. 120, pp. 234–241, Mar. 2015.

[8] R. M. M. Pereira, C. M. M. Ferreira, and F. M. Barbosa, "Comparative study of STATCOM and SVC performance on dynamic voltage collapse of an electric power system with wind generation," *IEEE Latin Amer. Trans.*, vol. 12, no. 2, pp. 138–145, Mar. 2014.

[9] T. Ding, R. Bo, H. Sun, F. Li, and Q. Guo, "A robust two-level coordinated static voltage security region for centrally integrated wind farms," *IEEE Trans. Smart Grid*, vol. 7, no. 1, pp. 460–470, Jan. 2016.

[10] J. Ouyang, T. Tang, Y. Diao, M. Li, and J. Yao, "Control method of doubly fed wind turbine for wind speed variation based on dynamic constraints of reactive power," *IET Renew. Power Gener.*, vol. 12, no. 9, pp. 973–980, Jul. 2018.

[11] Y. Su *et al.*, "Transient overvoltage control for a wind farm based on goal representation adaptive dynamic programming," in *Proc. Int. Conf. Power Syst. Technol.*, Oct. 2014, pp. 705–712.

[12] N. E. Karakasis and C. A. Mademlis, "High efficiency control strategy in a wind energy conversion system with doubly fed induction generator," *Renew. Energy*, vol. 125, pp. 974–984, Sep. 2018.

[13] D. Xie, Z. Xu, L. Yang, J. Ostergaard, Y. Xue, and K. Wong, "A comprehensive LVRT control strategy for DFIG wind turbines with enhanced reactive power support," *IEEE Trans. Power Syst.*, vol. 28, no. 3, pp. 3302–3310, Aug. 2013.

[14] J. Morren and S. W. H. de Haan, "Ridethrough of wind turbines with doubly-fed induction generator during a voltage dip," *IEEE Trans. Energy Convers.*, vol. 20, no. 2, pp. 435–441, Jun. 2005.

[15] Z. Dao and F. Blaabjerg, "Optimized demagnetizing control of DFIG power converter for reduced thermal stress during symmetrical grid fault," *IEEE Trans. Power Electron.*, vol. 33, no. 12, pp. 10326–10340, Dec. 2018.

[16] D. Zheng, X. Xiong, J. Ouyang, Z. Zhang, and C. Xiao, "Control method for maximizing fault voltage of wind generation-integrated power systems with consideration of DFIG–grid coupling," *IEEE Access*, vol. 7, pp. 894–905, 2019.

[17] Y. Mi, C. Ma, Y. Fu, C. Wang, P. Wang, and P. C. Loh, "The SVC additional adaptive voltage controller of isolated wind-diesel power system based on double sliding-mode optimal strategy," *IEEE Trans. Sustain. Energy*, vol. 9, no. 1, pp. 24–34, Jan. 2018.

[18] N. T. Linh, "Voltage stability analysis of grids connected wind generators," in *Proc. 4th IEEE Conf. Ind. Electron. Appl.*, Xi'an, China, May 2009, pp. 2657–2660.

[19] D. Dawei and Z. Guiping, "Power transmission characteristics of low voltage microgrids," *Trans. China Electrotech. Soc.*, vol. 25, no. 7, pp. 117–122, Jul. 2010.

[20] J. Hu, Y. He, L. Xu, and B. W. Williams, "Improved control of DFIG systems during network unbalance using PI–R current regulators," *IEEE Trans. Ind. Electron.*, vol. 56, no. 2, pp. 439–451, Feb. 2009.

[21] L. Qu and W. Qiao, "Constant power control of DFIG wind turbines with supercapacitor energy storage," *IEEE Trans. Ind. Appl.*, vol. 47, no. 1, pp. 359–367, Jan. 2011.

[22] N. Chen, L.-Z. Zhu, and W. Wang, "Strategy for reactive power control of wind farm for improving voltage stability in wind power integrated region," *Proc. CSEE*, vol. 29, no. 10, pp. 102–108, Apr. 2009.

[23] J. Ouyang and X. Xiong, "Research on short-circuit current of doubly fed induction generator under non-deep voltage drop," *Electr. Power Syst. Res.*, vol. 107, no. 2, pp. 158–166, Feb. 2014.

[24] A. Damdoum, I. Slama-Belkhodja, M. Pietrzak-David, and M. Debbou, "Low voltage ride-through strategies for doubly fed induction machine pumped storage system under grid faults," *Renew. Energy*, vol. 95, pp. 248–262, Sep. 2016.

[25] J. Yao, R. Liu, T. Zhou, W. Hu, and Z. Chen, "Coordinated control strategy for hybrid wind farms with DFIG-based and PMSG-based wind farms during network unbalance," *Renew. Energy*, vol. 105, pp. 748–763, May 2017.

[26] R. Tonkoski, L. A. C. Lopes, and T. H. M. El-Fouly, "Coordinated active power curtailment of grid connected PV inverters for overvoltage prevention," *IEEE Trans. Sustain. Energy*, vol. 2, no. 2, pp. 139–147, Apr. 2017.

[27] K. A. Shu *et al.*, "Wind Power Accommodation Based on Block Price," *Trans. China Electrotechnical Soc.*, vol. 32, pp. 39–49, Jul. 2017.

JINXIN OUYANG (M'15) received the B.E. and Ph.D. degrees in electrical engineering from Chongqing University, Chongqing, China, in 2012, where he is currently a Professor with the School of Electrical Engineering. His research interest includes analysis and the protection and control of renewable energy integrated power systems.

MENGYANG LI received the B.E. degree in electrical engineering from Chongqing University, Chongqing, China, in 2017, where she is currently pursuing the M.Sc. degree with the School of Electrical Engineering. Her research interests include wind power and the economic dispatch of power systems.

ZHEN ZHANG received the B.E. degree in electrical engineering from Chongqing University, Chongqing, China, in 2018, where she is currently pursuing the M.E. degree with the School of Electrical Engineering. Her research interest includes the protection and control of renewable energy integrated power systems.

TING TANG received the B.E. degree in electrical engineering from Wuhan University, Wuhan, China, in 2016. He is currently pursuing the M.Sc. degree with the School of Electrical Engineering, Chongqing University, China. His research interests include wind power and power system stability analysis.